Korean J. Chem. Eng., 32(1), 20-29 (2015)
DOI: 10.1007/s11814-014-0183-3

pISSN: 0256-1115
eISSN: 1975-7220

Analysis of the dynamics of a packed column using semi-empirical models: Case studies with the removal of hexavalent chromium from effluent wastewater

Somdutta Singha and Ujjaini Sarkar†

Department of Chemical Engineering, Jadavpur University, Kolkata-700032, West Bengal, India
(*Received 17 January 2014 • accepted 1 July 2014*)

Abstract−The dynamics of a packed bed, used for handling enormous quantities of effluent wastewater from industrial discharge, is a very important issue from a design point of view. Semi empirical Thomas and BDST Models are applied to analyze the dynamic behavior of packed beds filled in with GAC and PAC. Variations in breakthroughs with respect to exhaustion time, various bed depths, flow rates and influent solute concentrations are studied. The linearized BDST model gives very high values of R^2=0.9959 (for 20% breakthrough) and R^2=0.9578 (for 85% breakthrough), indicating the validity of the model for the present column system for both 20 and 85% of breakthroughs. For breakthroughs, below the 50% saturation, the BDST model is used to estimate the design of columns with various scale-ups of the process for other flow rates and initial adsorbate concentrations without any additional experiments. BDST coefficients of lower breakthroughs, below 50%, can also be used for evaluating other parameters such as critical bed depth, adsorption capacity and rate constant. The values of BDST constants, N_0 and K, are not affected by changing flow rates for a particular adsorbent combination and changing influent concentrations. The validity of the Thomas model is ensured by the high R^2 values, ranging from 0.855 to 0.925, while estimating the Thomas k_{Th} and q_0.

Keywords: BDST and Thomas Model, Column Dynamics, Critical Bed Depth, Packed Bed, Wastewater Treatment

INTRODUCTION

Chromium behaves as a hazardous contaminant in water and in the aqueous system. It is present in its soluble state in two forms: trivalent chromium [Cr(III)] and hexavalent chromium [Cr(VI)]. Between these two forms Cr(III) is a bio-element and it is considered as not harmful, rather an essential nutrient for human [1,2]. According to Kalidhasan et al. [3], Cr(III) is required in mammals for the metabolism of normal carbohydrate or glucose. On the other hand, Cr(VI) is 500 times more toxic than Cr(III) [4]. Health hazards related to water contaminated with Cr(VI) include gastric upset, ulcer, kidney and liver damage, changes to genetic materials, weakening the immune system, allergic reaction and rashes on the skin etc [5,6]. This causes a variety of diseases such as severe diarrhea, hemorrhage epigastric pain, affecting digestive organs, nausea and vomiting [1,7]. Therefore, the presence of Cr(VI) in the environment is of serious concern. This form of chromium poses carcinogenic, mutagenic and teratogenic features in biological systems, as indicated by Fendorf et al. [8] and Han et al. [9]. Both the natural and manmade sources are responsible for the water pollution generated by Cr(VI). Various industries like tanneries, steel industries, metal processing industries, chromium plating, dye and pigment preparation, textile industries, and wood preservation discharge a huge amount of wastewater containing chromium into the inland surface water body. On a long-term basis, this contaminates the water bodies as well as soil. Chromium contamination levels vary from 5 to 220 mg/L [10,11] depending on various industrial sources. Among various pretreatment processes, chemical precipitation, ion exchange, membrane filtration, solid phase and liquid-liquid extraction, adsorption [12-16] are effective for removal of Cr(VI) from the wastewater in order to protect the ecosystem and public health. Some drawbacks like high cost, incomplete removal of the metal, high-energy requirement or generation of high volume of sludge put a restriction on the application of these methods. Adsorption may be an effective and versatile method if less expensive adsorbents are used for removing chromium from wastewater, particularly when combined with appropriate regeneration steps. A column packed with suitable adsorbents can be used in a continuous mode for this removal process. Among various commercial adsorbents, activated carbon is one of the least expensive adsorbents for the treatment of wastewater [2]. Activated carbon is a carbonaceous material that has high levels of porosity, internal surface area and relatively high mechanical strength, which are some of the required characteristics for it to act as a good adsorbent. Many researchers [17-19] have shown that adsorption, using activated carbon, is a widely applied method, because of its economic viability and high removal efficiency. Dynamics of a packed bed filled with activated carbon is examined along with performance of the bed for the removal of Cr(VI) with the help of breakthrough curves. Successful design of this study requires prediction of the concentration-time profile for the effluent. Effect of various parameters like bed height, influent (wastewater flowing into the packed bed column defined as "influent flow") concentration and flow rate related to the breakthrough curves for a fixed bed column are tested. The maximum adsorption capacity of an adsorbent is also found, which is further used in the design of the packed column [20]. Apart

†To whom correspondence should be addressed.
E-mail: usarkar@chemical.jdvu.ac.in, abhi_nandan47@rediffmail.com

from the pore diffusion model [21], many semi empirical models are used to analyze the laboratory scale column in order to design pilot scale columns [22,23]. These semi empirical models are used for evaluating some more design parameters, which characterize the performance and capacity of adsorbent in a dynamic system. The theoretically predicted breakthrough curves obtained by these models are compared with corresponding experimental breakthrough curves. For the design of an adsorption column for various flow rates, bed height and influent concentrations, the experimentally obtained service times are compared with the theoretically predicted values obtained by the semi empirical models. There are a number of mathematical models for designing full-scale adsorption column. Amongst them, the most widely used models, which were previously mentioned by many authors, are *BDST* and *Thomas* models. To evaluate these models with the experimental data for some parameters of the packed bed dynamics, such as breakthrough and exhausted time, initial influent concentration (C_0), influent concentration at any time t (C_t), service time (service time refers to the time utilized by the adsorption column to reach the breakthrough point with specific saturation percentage), linear flow rate, bed height etc., need to be known.

In this study, we use a composite fixed bed where both powder activated carbon (PAC) and granular activated carbon (GAC) are used. Breakthrough curves for this packed column are examined by both BDST and Thomas models. Parameters like bed height, time, rate constant, and adsorption efficiency are evaluated by these two models, and model outputs are validated by a fresh set of experimental data. Lastly, up-gradation of the column for other flow rates and influent concentrations is also attempted with the help of these two models.

THEORETICAL BACKGROUND OF BDST AND THOMAS MODELS

1. BDST Model

The concept of bed depth service time (BDST) model, first proposed by Bohart and Adams [24] in 1920, has been regarded as the simplest semi-empirical model in the fixed bed analysis that enables most rapid prediction of adsorbent performance [25]. This model, based on surface reaction rate theory, therefore assumes that the rate of sorption is proportional to the fraction of sorption capacity remaining on the adsorbent [26,27]. This model can predict the relationship of bed depth (or height) of the fixed bed column with service time [28,29]. Validation of the model stands on the basic assumption that intra-particle diffusion and external mass transfer resistance are both negligible and that adsorption kinetics, controlled by the surface chemical reaction between the solute and the adsorbent, is rare in real systems [30]. The symmetry of the breakthrough curves, an assumption inherent in the BDST theory, is rarely found to be true in practice. This shows the limitation of this simple model [31]. The BDST model is practiced worldwide, though it suffers from certain limitations. The model is applicable only to describing the initial part of the breakthrough curve, approximately just up to the breakthrough point or 10-50% of saturation points [23]. The systems taking long time to reach equilibrium are not suitable for a basic BDST analysis. This is mainly because the solid-phase loading of the bed does not show a constant relationship with time at different bed heights of a column [32]. To eliminate this limitation a constant bed capacity throughout the column operation is assumed for the original BDST model, which may also not be true in most cases.

The original expression of BDST model, proposed by Bohart and Adams, is as follows:

$$\ln\left(\frac{C_0}{C_t}-1\right)=\ln[\exp^{KZN_0/v}-1]-KC_0t \tag{1}$$

where, C_0=Initial concentration of the solute in influent (mg/L)
C_t=Solute concentration in effluent at any time (mg/L)
K=Adsorption rate constant or BDST model constant (L/mg h)
Z=Bed depth or height (cm)
N_0=Adsorption capacity (mg/L)
v=Linear flow velocity (cm/h)
t=Service time (h)

The BDST model can be used to estimate few characteristic parameters like adsorption capacity (N_0), adsorption rate constant (K) of the fixed bed etc. Eq. (1) can be rearranged in a linear form to yield an expression for service time (t), proposed by Hutchins [33] as,

$$t=\frac{ZN_0}{C_0v}-\frac{1}{KC_0}\ln\left(\frac{C_0}{C_t}-1\right) \tag{2}$$

When, $\exp^{KN_0Z/v}>>1$ the BDST model can be used for both breakthrough point (breakthrough point is defined as the time in which a packed bed is maximum utilized so that it has low adsorption towards the effluent wastewater and the outlet from the bed has sudden increase in concentration than the initial adsorption) and exhausted point (the point on the breakthrough curve at which solute or adsorbate concentration reaches almost equal to the influent concentration is refereed as "exhausted points") of the breakthrough curve. If the service time at breakthrough point is t_b and service time at exhausted time is t_x with corresponding effluent solute concentrations being C_b and C_x respectively, then the two equations will be,

$$t_b=\frac{ZN_0}{C_0v}-\frac{1}{KC_0}\ln\left(\frac{C_0}{C_b}-1\right) \tag{3}$$

$$t_x=\frac{ZN_0}{C_0v}-\frac{1}{KC_0}\ln\left(\frac{C_0}{C_x}-1\right) \tag{4}$$

Both Eqs. (3) and (4) can be re-written in the form of a straight line,

$$t=aZ-b \tag{5}$$

where, slope=$a=\frac{N_0}{C_0v}$

And intercept=$b=\frac{1}{KC_0}\ln\left(\frac{C_0}{C_x}-1\right)$

Now plotting t versus Z of the bed for a fixed flow rate we get a straight line, and from the slope and intercept of this straight line we get the adsorption capacity (N_0) and adsorption rate constant (K), respectively. Different flow rates will give different straight lines

with different N_0 and K. This exactly means that the effect of flow rates upon bed performance can be studied by BDST model. Now the validity of the linearized form of the BDST model for a particular dynamic system can be established by the higher values of regression coefficients [34]. After getting the values of N_0 and K from the graph, the theoretical values of service time (t) for a specific bed height (Z) can be calculated from Eq. (2) and can be fitted as model data along with the experimental data over a range of flow rates.

There is a minimum bed depth required in an adsorbent column for a particular breakthrough concentration (C_b): the *critical bed depth* (Z_0) [23,35]. Z_0 is actually a theoretical bed depth of adsorbent column by which it can be ensured that the effluent solute concentration does not exceed the breakthrough concentration (C_b) at time t=0. So we can calculate Z_0 by putting t=0 in Eq. (2) and solving it in terms of Z_0. We get

$$Z_0 = \frac{v}{KN_0}\ln\left(\frac{C_0}{C_b}-1\right) \tag{6}$$

Therefore, this is another utility of using BDST model as we can calculate a minimum bed height required for a particular influent concentration and a specific flow rate. Now according to Vijayaraghavan et al. [36] critical bed depth will vary with the value of K. As long as the value of K is large, even a short bed will avoid breakthrough, but as K decreases, progressively longer bed is required to avoid breakthrough.

At 50% of the breakthrough curve where effluent solute concentration C_t is just half of the influent solute concentration C_0, that is $C_t=(1/2)C_0$, the logarithmic term in Eq. (2) becomes zero. Thus, and can be written as,

$$t_{50} = \frac{N_0}{C_0 v}Z \tag{7}$$

where, t_{50} is the service time at 50% of the breakthrough curve [31, 37]. From this expression, we can see that there is no intercept of the straight line. If t_{50} versus Z is a straight line that passes through the origin, it can be said that the adsorption data of the fixed bed follow the BDST model well.

An experimental run with one flow rate can be reliably scaled up for the other flow rates without further experiments [38,39]. This can be done by predicting the slope of the straight line of t versus Z plot of a new flow rate from the known slope of a previous one. If the previous flow rate is Q with slope a, then the new slope (a_1) of new flow rate (Q_1) will be obtained by the relation,

$$a_1 = a\cdot\left(\frac{Q}{Q_1}\right) \tag{8}$$

Here the intercept of the straight line (b) is not adjusted since this is not affected by changing flow rates but depends only on the influent solute concentration (C_0).

Designing the column with other influent solute concentrations can be done by one influent solute concentration using the BDST approach [40]. The slope and intercept of the known system are used to get new values of the slope and the intercept of changing influent concentration. If the a and b are the slope and intercept of the known system with the influent concentration C_1, respectively, then the new slope (a_2) and new intercept (b_2) of the influent concentration C_2 can be calculated by the following equations:

$$a_2 = a\cdot\left(\frac{C_1}{C_2}\right) \tag{9}$$

$$b_2 = b\cdot\left(\frac{C_1}{C_2}\right)\cdot\left[\frac{\ln\left(\frac{C_2}{C_F}-1\right)}{\ln\left(\frac{C_1}{C_B}-1\right)}\right] \tag{10}$$

where, C_F=effluent concentration at influent concentration C_2
C_B=effluent concentration at influent concentration C_1

2. Thomas Model

The Thomas model [41] describes the design, performance and dynamics of an adsorption column [42-44]. This model, derived from the second-order reversible reaction kinetics (the rate determining step), is followed by any adsorption system [45]. The basic assumption of the Thomas model is Langmuir kinetics of adsorption-desorption without any axial term [35,46]. The experimental can be fitted to the Thomas Model in order to obtain the maximum adsorption capacity of the packed bed column along with the kinetic rate constant [47,48].

General expression of the Thomas model is,

$$\frac{C_t}{C_0} = \frac{1}{1+\exp\left[\left(\frac{k_{Th}}{Q}\right)(q_0M - C_0V_{eff})\right]} \tag{11}$$

k_{Th}=Thomas rate constant (ml/min/gm)
Q=Flow rate (ml/min)
q_0=Maximum adsorption capacity of the adsorbent bed (mg/g)
M=Mass of the adsorbent (g)
V_{eff}=Volume of the effluent (ml)

The linearized form of the Thomas model is as follows:

$$\ln\left(\frac{C_0}{C_t}-1\right) = \frac{k_{Th}q_0M}{Q} - \frac{k_{Th}C_0V_{eff}}{Q} \tag{12}$$

Based on our previous discussions, the service time, $t=V_{eff}/Q$. So Eq. (12) can be re-written as,

$$\ln\left(\frac{C_0}{C_t}-1\right) = \frac{k_{Th}q_0M}{Q} - k_{Th}C_0t \tag{13}$$

From this linearized form of Eq. (11), plotting $\ln(C_0/C_t-1)$ versus t we get a straight line. So the Thomas rate constant (k_{Th}) and the maximum adsorption per gm of adsorbent (q_0) can be calculated from the slope and the intercept of the straight line, respectively. Predicted data are correlated to the experimental data and the nature of breakthrough curves can be estimated by the fitness of the model line. The main drawback of this model is that it is derived from second-order reversible reaction kinetics, whereas physical adsorption is not chemical reaction kinetics always, rather controlled mostly by the inter phase mass transfer [20,49]. Thus, when this model is used for a physical adsorption process in a packed bed column, it can develop some error. On the other hand, cases with chemisorption may be well validated by the Thomas Model.

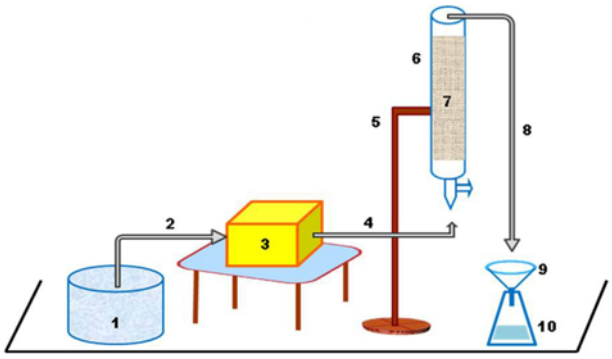

Fig. 1. Experimental setup for the packed bed column made by combination of GAC and PAC in a ratio of 9 : 1 for the removal of Cr(VI).

1. Storage tank of Cr(VI) solution
2. Delivery line
3. Peristaltic pump
4. Influent flow of wastewater
5. Column stand
6. Glass column
7. Packing materials
8. Effluent outlet
9. Funnel
10. Sample collecting apparatus

MATERIALS AND METHODS

1. Materials

Artificial wastewaters of this experiment were prepared in our laboratory. We prepared Cr(VI) solution by dissolving potassium di-chromate ($K_2Cr_2O_7$) in double distilled water. We tried to prepare stock solution of Cr(VI) for our experiment for a range of 10 to 50 mg/L. All chemicals and commercial adsorbents (PAC and GAC) used were of analytical reagent grade and purchased from MERCK and SD Fine Chemicals.

2. Experimental Design

The experiments for continuous adsorption of wastewater are conducted in a glass column of internal diameter 24 mm and a length of 30 cm. A storage tank, a pumping arrangement with a peristaltic pump and a distribution system (*see* Fig. 1) are the accessories of the treatment system. The column is packed with known quantity of GAC and PAC in a 9 : 1 ratio in order to obtain a particular bed depth of the column. This packed column is supported by cotton on both sides of the packing, where a blob of cotton provided the support of the packed bed as well as maintained a uniform distribution of the wastewater along the packed bed. The cotton at the top of the bed prevents the washout of adsorbent materials along with the outgoing stream of the treated wastewater. The inlet of the adsorption column is equipped with a distribution system in order to get uniform flow across the cross section of the adsorption column. The simulated wastewater containing Cr(VI) is fed through the fixed-bed column in an up-flow mode to avoid channeling and flooding of the effluent and unnecessary compaction of the bed. Before the operation, the bed is rinsed with distilled water and left overnight to ensure a closely packed arrangement of particles with no additional voids, channels, or cracks. A peristaltic pump (Make: Masterflex C/L, Model no. 77122-00) is used to control the flow rate at the inlet and outlet.

3. Operational Condition

Other variables for the breakthrough curve analysis are bed depths (8, 16 and 24 cm), influent concentrations (10, 20 and 30 mg/L) and flow rates (1.53, 2.45 and 3.07 mL/s). The wastewater is treated until the ratio C_t/C_0=0.85. The experiments are carried out at different flow rates, feed concentrations and bed heights without changing the ratio of the adsorbents. Wastewater was coming out from the column collected at every 20 min interval and then was analyzed for Cr(VI) concentration. So the changes of concentration after every 20 min were measured by spectroscopic method.

4. Analytical Procedure

A spectrophotometer [Make: PERKIN ELMER; Model: PRECISELY LAMDA 25 UV/Visible; Range of wavelength: 330-900 nm], equipped with a standard 10 nm path length sample cell, is used for absorption measurements of Cr(VI). Cr(VI) is determined by spectrophotometric method where reaction with 1-5 di-phenyl carbazide (DPC) in an acidic solution can produce a violet colored (magenta chromagen) complex, absorbing light at λ=540 nm, as per standard methods [50]. Here, the required amount of filtrate (after adsorption) is taken in a 50 ml graduated make-up flask by eppendorf automated pipette and the volume is made up with ultra pure water. Concentrations of Cr(VI), in each solution, are calculated from a standard curve already developed. Sulfuric acid is added prior to the addition of DPC to lower the pH of the solution.

RESULTS AND DISCUSSION

In a fixed bed, during the adsorption process, required concentration gradients between adsorbent and adsorbate are always available as the adsorbate is continuously in contact with a given quantity of fresh adsorbent [51,52]. The design and theory of fixed-bed adsorption systems focuses on establishing the shape of the breakthrough curve [44]. Also, the breakthrough times and bed volumes are used in the evaluation of the performance of a fixed-bed column [53,54]. Mostly three important parameters influence the breakthrough curve in a dynamic system: the flow rates, bed height and inlet concentration of the solute. The performance of the bed is thus studied with respect to the effects of changing flow rates, bed heights and an inlet concentration (feed concentration) until the breakthrough time is reached. At the initial part when the bed was completely unsaturated maximum adsorption capacity of the bed remained near about 20% of the total concentration of Cr(VI). So there is a point in the breakthrough curve from which curve got its first break at C_t is 20% of C_0 (C_t/C_0=0.2) and this is called the "breakthrough point." Similarly, when the C_t is increased and reached its maximum where no more adsorption capacity of the bed was left, the breakthrough curve again changed, and this point is called the "exhausted point." In our experiment it came at the time when C_t was 85% of C_0 (C_t/C_0=0.85) and is called the "point of exhaustion".

1. Effect of Bed Depth on Breakthrough Curve

The effect of bed depth (varying from 10 to 30 cm) on the packed bed column was investigated, keeping the influent solute concentration and flow rate fixed at 10 mg/L and 1.53 mL/s respectively. The ratio of effluent solute concentration (C_t) at time t and the influent solute concentration (C_0) were plotted against the service time (t). C_t/C_0 versus t plot is known as a breakthrough curve. The breakthrough curve of varying bed depth is presented in Fig. 2. From Fig. 2 we can see that the shape and gradient of each curve is dif-

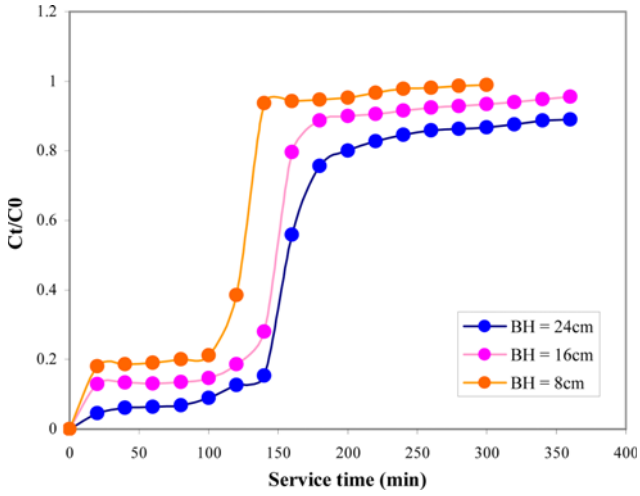

Fig. 2. Break through curves for the dynamic study for removal of hexavalent chromium by composite bed at various bed heights maintaining a constant inlet concentration and a constant flow rate.

ferent with variation of bed depth. Maximum Cr(VI) uptake is observed at the beginning of the fixed bed, but the removal decreases as time progresses. The lower the bed depth is, it is saturated earlier than a bed with higher bed depth as more adsorbent materials are present in the column with a higher depth. Amounts of adsorbent (activated carbon) present in the 8, 16 and 24 cm columns are 20, 40 and 60 gms, respectively. The longer column (24 cm) contained more adsorbent than the shorter one (8 cm), so more adsorbing sites are available in the column with higher bed depth. Thus, adsorption capacity is increasing with increase in the bed depths. Apart from the availability of more adsorption sites, higher contact time is also available in a longer bed for Cr(VI) adsorption than in beds with lower bed height. Due to the longer contact time and availability of huge number of adsorption sites, the breakthrough comes later in case of column with higher bed depth than with a lower one. Therefore, for the column with bed height 8 cm, breakthrough curve is much stiffer than for the column with height 24 cm.

2. Effect of Flow Rate on Breakthrough Curve

Columns were run at various flow rates of 1.53, 2.45 and 3.07 mL/s with a fixed bed height of 24 cm and an influent concentration of 10 mg/L to study the effect of flow rate in the performance of the packed bed. The results are shown in the Fig. 3. The results indicate that with the increase of flow rates at a constant bed depth and fixed influent concentration the service time of breakthrough curves decrease. This is because, with the increase of flow rate the residence time of the bed decreases, which lowers the removal efficiency of the packed bed. At higher flow rate when the velocity is high, the mass transfer rate increases and due to this, equilibrium time of adsorption would come faster. On the other hand, low flow rate with relatively lower velocity would shift the depth of the adsorption zone and mass transfer zone to the lower end. As the adsorbent of packed bed needs sufficient time to bind Cr(VI), low flow rates with high bed contact time are effective for the removal of Cr(VI). Packed beds with low flow rate take longer time to be saturated and reach breakthrough, as the adsorption zone moves slowly to the top of the column, which increases the contact time for adsorption.

3. Effect of Influent Solute Concentration on Breakthrough Curve

The effect of influent solute concentration was evaluated with three initial feed solutions of 10, 20 and 30 mg/L keeping the bed height fixed at 24 cm and flow rate 1.53 mL/s. The breakthrough curves of these variable feed concentrations are shown in Fig. 4. The service time of these curves decreases with increasing influent solute concentrations. From the result we can say, the adsorbent bed is saturated faster for higher influent concentration. Probably because of non-linear interferences in adsorption, the breakthrough comes later with lower Cr(VI) concentration. This non-linear ad-

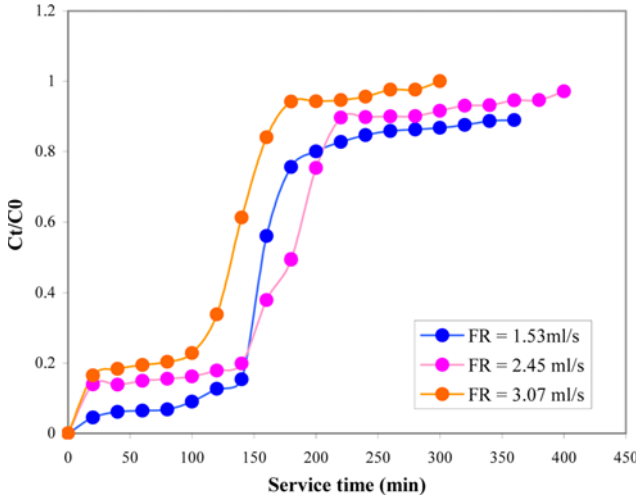

Fig. 3. Breakthrough curves for the dynamic study for removal of hexavalent chromium by composite bed at different flow rates maintaining a constant bed height and constant inlet concentration.

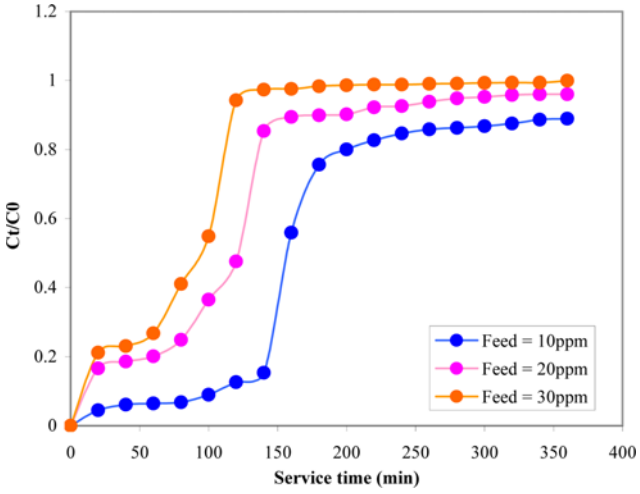

Fig. 4. Breakthrough curves for the dynamic study for removal of hexavalent chromium by composite bed at various inlet concentrations maintaining a constant bed height and a constant flow rate.

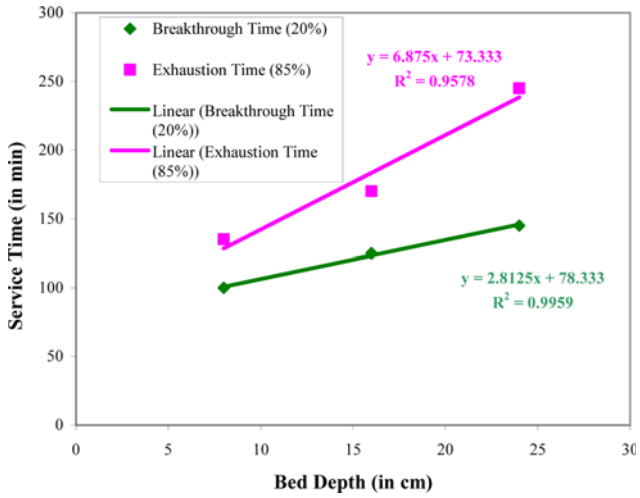

Fig. 5. Bed depth vs. service time plot at breakthrough time (20%) and exhausted time (85%) in fixed bed column for the removal of hexavalent chromium.

sorption behavior is a common feature in fixed bed analysis where the values of (C_t/C_0) are higher at low influent concentration than with high influent concentrations.

4. Application of BDST Model

From the breakthrough times (corresponding to C_t/C_0=0.2) and the exhausted times (corresponding to C_t/C_0=0.85) for the bed depths of 8, 16 and 24 cm, a graph of service time (t) versus bed depth (Z) is plotted, as seen in Fig. 5. For 20% and 85% saturation of the column, required times are found for each of the column bed depths using Fig. 2. From the plot of Fig. 5 two straight lines for 20% and 85% saturation are drawn and the equations of these lines are as follows:

$$t_b=2.8125z+78.333 \text{ (for 20\% saturation of } C_t/C_0) \quad (14)$$

$$t_x=6.875z+73.333 \text{ (for 85\% saturation of } C_t/C_0) \quad (15)$$

These two straight lines are experimentally obtained and predictions for other flow rates and other influent concentrations can be estimated by using equations of these two lines.

4-1. Analysis of BDST Model: Variation of Bed Depth

From Eqs. (14) and (15), which are obtained experimentally, the predicted values of breakthrough time (t_b) and exhausted time (t_{ex}) for the varying bed depth (8 to 24 cm) with flow rate 1.53 ml/s and an influent concentration of 10 mg/L were calculated and both the experimental and predicted values are presented in Table 1. From the data of Table 1, the predicted values for both of t_b and t_{ex} (for each of the bed depths) are in good agreement with the experimental values. Close matches of the predictions by the BDST model with the experimental values suggested that the BDST model could be acceptable for this packed bed system. Linear relationships of these two Eq. (14) and (15) are obtained with R^2=0.9959 (for 20% saturation) and 0.9578 (for 85% saturation). These high values of R^2 indicate the validity of the BDST model for the present column system for both 20 and 85% of breakthroughs.

The adsorption capacity (N_0) and the BDST rate constant (K) were then calculated from the slope and the intercept of Eq. (2) and (3), respectively, for both the 20% and 85% of C_0. The values

Table 1. Comparison between experimental and predicted values of breakthrough time (t_b) and exhausted time (t_{ex}) for various controlling parameters of packed bed column like bed depth, flow rate and influent concentration by BDST Model

Fixed parameter	Variable parameter	Breakthrough time (t_b) at 20% C_t/C_0 (in min) [experimental]	Breakthrough time (t_b) at 20% C_t/C_0 (in min) [predicted]	Exhausted time (t_{ex}) at 85% C_t/C_0 (in min) [experimental]	Exhausted time (t_{ex}) at 85% C_t/C_0 (in min) [predicted]
Q=1.53 ml/s	Z=8 cm	100	100.87	135	128.33
C_0=10 mg/L	Z=16 cm	125	123.41	170	183.33
	Z=24 cm	143	145.95	240	238.33
Z=24 cm	Q=2.45 ml/s	140	120.48	211	176.36
C_0=10 mg/L	Q=3.07 ml/s	90	111.97	160	155.55
Q=1.53 ml/s	C_0=20 mg/L	60	72.91	140	119.15
Z=24 cm	C_0=30 mg/L	18	48.60	115	79.43

Table 2. Predictions of N_0 and K for the other flow rates and other influent concentrations, the scale up processes at different flow rates and influent concentrations by BDST model analysis

Analysis	Fixed parameter	Scaling up parameters	Breakthrough at 20% C_t/C_0		Exhausted at 85% C_t/C_0		Linear flow rate v (cm/h)	Critical bed depth Z_0 (cm)
			N_0 (mg/L)	K (L/mg h)	N_0 (mg/L)	K (L/mg h)		
Experimental	C_0=10 mg/L; Z=8-24 cm	Q=1.53 ml/s	34260.47	−0.0017	83747.81	0.0024	1218.15	−27.85
Predicted	C_0=10 mg/L; Z=8-24 cm	Q=2.45 ml/s	34260.86	−0.0017	83740.55	0.0024	1950.63	−44.60
Predicted	C_0=10 mg/L; Z=8-24 cm	Q=3.07 ml/s	34258.88	−0.0017	83740.69	0.0024	2444.27	−55.89
Predicted	Q=1.53 mL/s; Z=8-24 cm	C_0=20 mg/L	34254.38	−0.0017	83735.63	0.0024	1218.15	-
Predicted	Q=1.53 mL/s; Z=8-24 cm	C_0=30 mg/L	34242.19	−0.0017	83723.45	0.0024	1218.15	-

of N_0 and K for the three bed depths with flow rate 1.53 ml/s and influent concentration 10 mg/L (calculated using BDST approach) are presented in Table 2. There was a rise in slopes about 2.5 fold from 2.8125 to 6.875 for a change in breakthrough from 20% to 85% saturation, evidenced from Eqs. (14) and (15). From Table 2 a subsequent increase in corresponding N_o from 34260.47 to 83747.81 mg/L was observed. This can be explained by the fact that there are more active sites of the GAC and PAC present, which are unoccupied by Cr(VI) ions at lower breakthrough (20% of C_t/C_0) value and thus the adsorbent remained unsaturated. The dynamic adsorption capacity in such low breakthrough condition is therefore bound to be lower than the full bed capacity of the adsorbent. Goel et al. [39] reported an increase in the magnitude of slope from 12.5 to 35 at breakthrough values of 20-60% Similar fact was also observed by Sharma and Forster [22] with an increase in slope by 4.72-fold from a breakthrough of 30-70% on removal of Cr(VI) by activated carbon. The rate constant for the 20% breakthrough is –0.00177, which is also very low with respect to the rate constant of 0.0024 for the 85% breakthrough. The lower rate constant at 20% saturation also suggested the lower adsorption capacity at 20% than at the 85% saturation.

The critical bed depth, (Z_0) for this packed bed system, with a flow rate of 1.53 ml/s and an influent concentration of 10 mg/L, was calculated from Eq. (6) for 20% breakthrough and the values are shown in Table 2. The critical bed depth (Z_0) is –27.85 cm, showing that the present bed depth is sufficient for the adsorption zone to produce an effluent within the 20% of C_0 limit with this operational condition. Another way to examine the application of the BDST model is to check the 50% breakthrough curve. According to Eq. (7), the curve for 50% breakthrough should pass through the origin. But the result is not satisfactory as the intercept obtained here is 111.67, which is quite a high value for the present operational conditions, proving the non-conformity of the BDST model with the adsorption of Cr(VI) by activated carbon at 50% breakthrough curve. Similar case of non-conformity on BDST with respect to 50% breakthrough on removal of Cr(VI) and total chromium by leaf mould and activated carbon and PANI-jute is also reported by Sharma and Forster [22] and Kumar and Chakraborty [40], respectively. All these experimental details, along with the findings from scientific literature, suggested that it is not necessary for the BDST model to be validated for higher breakthrough percentages. Therefore, BDST coefficients of lower breakthroughs, below 50%, can still be utilized for evaluating other parameters such as critical bed depth, adsorption capacity and rate constant. Also, lower breakthroughs, below 50%, can be estimated using the BDST model to design columns with different scale ups for processes with other flow rates and initial adsorbate concentrations without further experiments.

4-2. Validation of BDST Model for Various Flow Rates

The parameters of a fixed adsorbent bed, obtained from experimental observations, are used for the design of an adsorption column for practical use. To investigate the scale up process by the BDST method, a new column with the same bed depth (24 cm) and influent concentration (10 mg/L) was operated at two different flow rates of 2.45 and 3.07 mL/s. The validity of the BDST model could be tested for the prediction of these two different flow rates from the experimental data of a third and unique flow rate. These experimentally obtained values of t_b and t_{ex} were compared with the predicted values of t_b and t_{ex} for different flow rates. If the slope of the experimental data is known, the slopes for other flow rates are easily calculated by applying Eq. (8). The value of the intercept is not affected significantly by flow rate, so the adjustment in the intercept is not required. For flow rates of 2.45 and 3.07 ml/s the equation of service time and bed depth can be written as,

For flow rate=2.45 ml/s,

$$t_b=1.7564z+78.333 \text{ (for 20\% saturation of } C_t/C_0) \quad (16)$$

$$t_x=4.923z+73.333 \text{ (for 85\% saturation of } C_t/C_0) \quad (17)$$

For flow rate=3.07 ml/s,

$$t_b=1.4016z+78.333 \text{ (for 20\% saturation of } C_t/C_0) \quad (18)$$

$$t_x=3.426z+73.333 \text{ (for 85\% saturation of } C_t/C_0) \quad (19)$$

Slopes and intercepts obtained from the Eqs. (16) to (19) were used to calculate the t_b and t_{ex} for the flow rates of 2.45 and 3.07 ml/s. These predicted values, along with the corresponding observed values, are shown in Table 1 for comparison between theoretical and experimental values. It could be said from Table 1 that the experimental values are at par with the theoretical values for both the breakthroughs of 20% and 85%. This means that BDST model is effective in predicting the scale-up of processes with varying flow rates.

The N_0 and K values could also be calculated from the predicted slopes and intercepts of the straight line for higher flow rates, and these values are given in Table 2. From the values of Table 2, there is almost no difference of N_0. For 20% breakthrough; there is only a decrease of N_0 from 34260.47 to 34258.88 mg/L, and for 85% breakthrough, the decrease is from 83747.81 to 83740.69 mg/L. The corresponding K values are same for both 20% and 85% breakthrough for all the flow rates. From these results, it is concluded that N_0 and K would not be affected by changing flow rates for a particular adsorbent combination. The Z_0 values were also calculated and shown in Table 2 from the predicted slopes and intercept of the two flow rates. Therefore, the advantage of the BDST model is that any experimental outcome could be reliably scaled up for other flow rates without undertaking a new set of experiments.

4-3. Validation of BDST Model for Various Initial Concentrations

It is also proposed that the data collected from one influent solute concentration could be adjusted by the BDST approach for designing systems for other influent solute concentrations. The degree of predictability for different initial concentrations of Cr(VI) by BDST model was checked by running the column with two different influent concentrations of Cr(VI), 20 and 30 mg/L, at a fixed flow rate of 1.53 ml/s and column bed depth of 24 cm. Theoretical t_b and t_{ex} are obtained from previous column study, conducted at a flow rate of 1.53 ml/s with the same depth of 8 cm and influent concentration [Cr(VI)] of 10 mg/L. Using Eq. (9) and (10), theoretical slopes and intercepts were calculated and breakthrough times were evaluated (Table 1) for an initial Cr(VI) concentration of 20 and 30 mg/L, respectively. With these values of slope and intercept, the equation of service time and bed depth can be written as,

For an influent concentration=20 mg/L,

$$t_b=1.406z+39.166 \text{ (for 20\% saturation of } C_t/C_0) \quad (20)$$

t_x=3.437z+36.666 (for 85% saturation of C_t/C_0) (21)

For an influent concentration=30 mg/L,

t_b=0.937z+26.111 (for 20% saturation of C_t/C_0) (22)

t_x=2.291z+24.444 (for 85% saturation of C_t/C_0) (23)

From Table 1 the theoretical and experimental values are well comparable for an influent concentration of 20 mg/L, but the theoretical values deviated from experimental values for 30 mg/L concentration. With the increase in influent Cr(VI) concentration from 20 to 30 mg/L corresponding, 20% breakthrough time decreased from 60 to 18 min. At higher influent Cr(VI), the fixed-bed was saturated with chromate ions more quickly, thereby decreasing the breakthrough t_b and t_{ex}. The N_0 and K values were calculated from the predicted slopes and intercepts of the straight line (Refer to Eqs. (20) to (23)) for other influent concentrations (see Table 2). N_0 corresponding to higher influent concentration is changed only a little bit, as compared to the previous value corresponding to the influent concentration of 10 mg/L. The value of N_0 at 20% breakthrough for 20 and 30 mg/L is 34,254.38 and 34,242.19 mg/L, respectively, whereas the experimental value is 34,260.47 mg/L. The N_0 value for 85% breakthrough decreased from 83,747.81 mg/L (experimental) to 83,735.63 (predicted) for an inlet concentration of 20 mg/L. The same reduced from 83,747.81 mg/L (experimental) to 83,723.45 mg/L (predicted) for an inlet concentration of 30 mg/L. There was no change in K values with the changing influent concentrations for this particular combination. Therefore, application of BDST model is successful to scale up the process to accommodate higher influent concentrations.

5. Application of Thomas Model

The linearized form of the Thomas model, $\ln(C_0/C_t-1)$ versus t, was used to estimate the two unknown parameters k_{Th} and q_0 of the Thomas equation. The estimated values of the Thomas parameters and the regression coefficient (R^2) of the linear form of the plots are listed in Table 3. The values of R^2 (ranging from 0.855 to 0.925) indicate that the results of the linear plot are easily acceptable. We can also see from the table that maximum adsorption capacity of the adsorbent bed is also very encouraging, although the rate constant is quite low.

5-1. Validation of Experimental Data by Thomas Model

The comparison of experimental and predicted breakthrough curves obtained at various bed depths, flow rate and influent solute concentration was tested. It could be seen from the figures that all the breakthrough curves are predicted quite well by the Thomas

Table 3. Adsorption capacity (q_0) and Thomas rate constant (k_{Th}) or various operational conditions

Fixed parameter	Variable parameter	k_{Th} (ml/min/gm)	q_0 (mg/g)	R^2
Q=1.53 ml/s	Z=8 cm	0.00261	75.96	0.8876
C_0=10 mg/L	Z=16 cm	0.00182	54.996	0.8553
	Z=24 cm	0.00183	47.892	0.8726
Z=24 cm	Q=1.53 ml/s	0.00183	47.892	0.8726
C_0=10 mg/L	Q=2.45 ml/s	0.00163	67.746	0.9145
	Q=3.07 ml/s	0.00251	57.372	0.9256
Q=1.53 ml/s	C_0=10 mg/L	0.00183	47.892	0.8726
Z=24 cm	C_0=20 mg/L	0.000805	52.223	0.8642
	C_0=30 mg/L	0.00076	41.582	0.8597

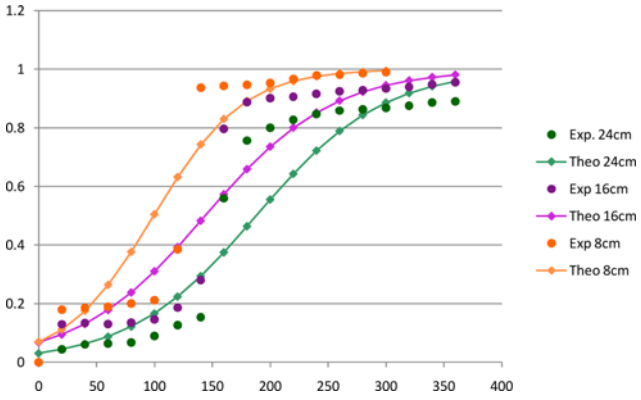

Fig. 6. Comparison of experimental and predicted (Thomas model) breakthrough curve obtained at three different bed depth 24, 16 and 8 cm keeping the flow rate and influent concentration constant at 1.53 ml/s and 10 mg/L respectively.

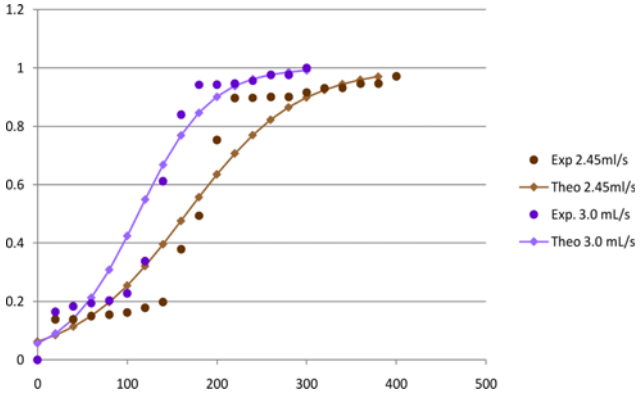

Fig. 7. Comparison of experimental and predicted (Thomas model) breakthrough curve obtained at different flow rates 2.45 and 3.07 mL/s, keeping the bed depth and influent concentration constant at 24 cm and 10 mg/L respectively.

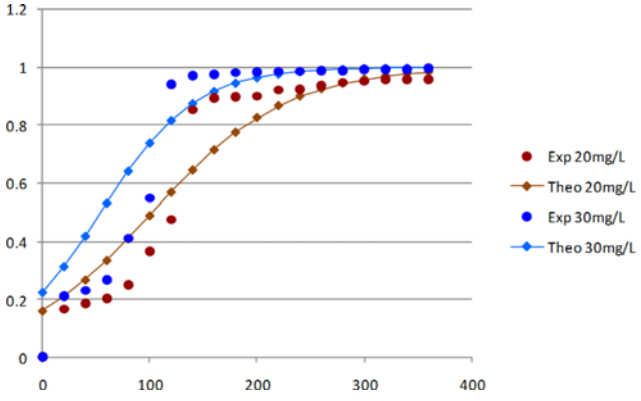

Fig. 8. Comparison of experimental and predicted (Thomas model) breakthrough curve obtained at different influent concentrations 20 and 30 mg/L, keeping the bed depth and flow rate constant at 24 cm and 1.53 mL/s respectively.

model. The dynamic behaviors of the column predicted with the Thomas model are shown in Figs. 6 to 8 with the experimental results (indicated by markers) and the theoretical calculated points (given as lines) for each parameter. It appears that the simulation of the whole range of breakthroughs for all flow rates and inlet concentrations studied is effective with the Thomas model, and the breakthrough curves computed from this model are in good agreement with experimental data for all types of operating conditions studied (refer Table 3). This model is one of the most general and widely used theoretical methods to describe column performance. The suitability of the Thomas model may be tested by the basic assumptions of this model: the external and internal diffusions are not the limiting step; Langmuir kinetics of adsorption-desorption is valid; no axial dispersion is present during the adsorption. However, adsorption is usually not limited by chemical reaction kinetics, but is often controlled by interphase mass transfer and the effect of axial dispersion may be important especially at lower flow rates. This discrepancy can generate some errors while modeling the adsorption process in the sorbate-sorbent systems.

CONCLUSION

Semi empirical Thomas and BDST models were applied to analyze the transient behavior of packed beds filled in with GAC and PAC in terms of variations in breakthroughs with respect to exhaustion time, various bed depths, flow rates and influent solute concentrations. Application of BDST model is successful to scale up a dynamic process to accommodate higher influent concentrations, other than those used to parameterize the model. The validity of Thomas model is ensured by the high R^2 values ranging from 0.855 to 0.925, while estimating the Thomas k_{Th} and q_0.

Linearized BDST model gives very high values of R^2=0.9959 (for 20% breakthrough) and R^2=0.9578 (for 85% breakthrough), indicating the validity of the model for the present column system for both 20 and 85% of breakthroughs. Here we can also calculate the BDST rate constant at different saturation points of the breakthrough curve. The rate constant of the 20% breakthrough is −0.00177, which is also very low with respect to the rate constant of 85% breakthrough being 0.0024. This low rate constant at 20% saturation suggested lower adsorption capacity of the bed at 20% than at 85% saturation. From the lower breakthroughs, below the 50% saturation, the BDST model can be used to estimate the design of columns with various scale-ups of the process for other flow rates and initial adsorbate concentrations without any additional experiments. Along with this, BDST coefficients of lower breakthroughs, below 50%, can also be utilized for evaluating other parameters such as critical bed depth, adsorption capacity and rate constant. The values of N_0 and K would not be affected by changing flow rates for a particular adsorbent combination. There are also no changes in the values of K with the changing influent concentrations for the GAC-PAC combination.

The simulation of the whole range of breakthrough curves for all the flow rates and inlet concentrations studied is effective with the Thomas model. The breakthrough curves computed from this model are in good agreement with experimental data for all the types of operating conditions studied. The validity of Thomas model for the GAC-PAC system is ensured by the high R^2 values ranging from 0.855 to 0.925.

ACKNOWLEDGEMENTS

The authors acknowledge the research grant provided by the Department of Science and Technology (DST), India under their Water Technology Initiative (WTI) Programme and Council of Scientific and Industrial Research (CSIR) who have provided the research scholar grant.

NOMENCLATURE

Symbol

a : slope of straight line obtained by BDST model [-]
b : intercept of straight line obtained by BDST model [-]
C_O : initial concentration [mg/L]
C_B : effluent concentration at influent concentration C_1 [mg/L]
C_b : effluent concentration at breakthrough time [mg/L]
C_F : effluent concentration at influent concentration C_2 [mg/L]
C_t : solute concentration in effluent at any time [mg/L]
C_x : effluent concentration at exhausted time [mg/L]
K : BDST model rate constant [L/mg h]
k_{Th} : thomas rate constant [ml/min/gm]
m : mass of the adsorbent [gm]
N_0 : adsorption capacity [mg/L]
Q : flow rate [ml/min or ml/s]
t : time or service time [min or h]
t_b : time at breakthrough point [min]
t_x : time at exhausted point [min]
t_{50} : service time at 50% of the breakthrough curve [min]
V_{eff} : volume of the effluent [ml]
Z : bed depth or height [cm]
Z_0 : critical bed depth [cm]
ν : linear flow velocity [cm/h]

REFERENCES

1. G. Rojas, J. Silva, J. A. Flores, A. Rodriguez and M. Ly Maldonado, *Sep. Purif. Technol.*, **44**, 31 (2005).
2. J. Acharya, J. N. Sahu, B. K. Sahoo, C. R. Mohanty and B. C. Meikap, *Chem. Eng. J.*, **150**, 25 (2009).
3. S. Kalidhasan, M. Ganesh, S. Sricharan and N. Rajesh, *J. Hazard. Mater.*, **165**, 886 (2009).
4. M. Costa, *Toxcol. Appl. Pharm.*, **188**, 1 (2003).
5. S. S. Baral, S. N. Das, P. Rath and R. Chaudhury, *Biochem. Eng. J.*, **34**, 69 (2007).
6. S. Srivastava, A. H. Ahmad and I. S. Thakur, *Bioresour. Technol.*, **98**, 1128 (2007).
7. L. Dupont and E. Guillon, *Environ. Sci. Technol.*, **37**, 4235 (2003).
8. S. Fendorf, B. W. Wielinga and C. M. Hansel, *Int. Geol. Rev.*, **42**, 691 (2000).
9. X. Han, Y. S. Wong, M. H. Wong and N. F. Y. Tam, *J. Hazard. Mater.*, **146**, 65 (2007).
10. S. K. Ouki and R. D. Neufeld, *J. Chem. Technol. Biotechnol.*, **70**, 3 (1997).

11. H. S. Altundogan, *Process. Biochem.*, **40**, 1443 (2005).
12. X. Zhou, T. Korenaga, T. Takahashi, T. Moriwake and S. Shinoda, *Water Res.*, **27**, 1049 (1993).
13. H. Shaalan, M. Sorour and S. Tewfik, *Desalination*, **14**, 315 (2001).
14. S. Rengaraj, C. K. Joo, Y. Kim and J. Yi, *J. Hazard. Mater.*, **102**, 257 (2003).
15. O. A. Fadali, Y. H. Magdy, A. A. M. Daifullah, E. E. Ebrahiem and M. M. Nassar, *J. Environ. Sci. Health Part A, Toxic/ Hazard Subst. Environ. Eng.*, **39**, 465 (2004).
16. N. Rajesh, R. K. Jalan and P. Hotwany, *J. Hazard. Mater.*, **150**, 723 (2008).
17. N. Zhao, N. Wei, J. Li, Z. Qiao, J. Cui and F. He, *Chem. Eng. J.*, **115**, 133 (2005).
18. A. El-Nemr, A. Khaled, O. Abdelwahab and A. El-Sikaily, *J. Hazard. Mater.*, **152**, 263 (2008).
19. D. Duranoglu, A. W. Trochimczuk and U. Beker, *Chem. Eng. J.*, **187**, 193 (2012).
20. E. Malkoc and Y. Nuhoglu, *Chem. Eng. Sci.*, **61**, 4363 (2006).
21. T. W. Weber and R. K. Chakravorti, *AIChE J.*, **20**, 228 (1974).
22. D. C. Sharma and C. E. Forster, *Process. Biochem.*, **31**, 213 (1996).
23. V. Sarin, T. S. Singh and K. K. Pant, *Bioresour. Technol.*, **97**, 1986 (2006).
24. G. Boharts and E. N. Adam, *J. Am. Chem. Soc.*, **42**, 523 (1920).
25. G. McKay and M. J. Bino, *Water Environ. Pollut.*, **66**, 33 (1990).
26. T. R. Muraleedharan, L. Philip and L. Iyenger, *Bioresour. Technol.*, **49**, 179 (1994).
27. M. Lehman, A. I. Zouboulis and K. A. Matis, *Environ. Pollut.*, **113**, 121 (2001).
28. D. Kratochvil and B. Volesky, *Water Res.*, **34**, 3186 (2000).
29. K. Vijayaraghavan and D. Prabu, *J. Hazard. Mater.*, **137**, 558 (2006).
30. S. Ayoob, A. K. Gupta and P. B. Bhakat, *Sep. Purif. Technol.*, **52**, 430 (2007).
31. Z. Zulfadhly, M. D. Mashitan and S. Bhatia, *Environ. Pollut.*, **112**, 463 (2001).
32. D. C. K. Ko, J. F. Porter and G. McKay, *Chem. Eng. Sci.*, **55**, 5819 (2000).
33. R. Hutchins, *J. Chem. En. Lond.*, **81**, 133 (1973).
34. M. Kobya, *Bioresour. Technol.*, **91**, 317 (2004).
35. N. Sankararamakrishnan, P. Kumar and V. S. Chauhan, *Sep. Purif. Technol.*, **63**, 213 (2008).
36. K. Vijayaraghavan, J. Jegan, K. Palanivelu and M. Velan, *Chem. Eng. J.*, **106**, 177 (2005).
37. S. Netpradith, P. Thiravetyan and S. Towprayoon, *Water Res.*, **38**, 71 (2004).
38. M. Z. Othman, F. A. Roddick and R. Snow, *Water Res.*, **35**, 2943 (2001).
39. J. Goel, K. Kachrvehi, C. Rajagopal and V. K. Garg, *J. Hazard. Mater.*, **125**, 211 (2005).
40. P. A. Kumar and S. Chakraborty, *J. Hazard. Mater.*, **162**, 1086 (2009).
41. H. C. Thomas, *J. Am. Chem. Soc.*, **66**, 1466 (1944).
42. Z. Aksu and F. F. Cagatay, *Sep. Purif. Technol.*, **48**, 24 (2006).
43. R. Han, Y. Wang, W. Yu, W. Zou, J. Shi and H. Lui, *J. Hazard. Mater.*, **139**, 513 (2006).
44. E. I. Unuabonah, B. I. Olu-Owolabi, E. I. Fasuyi and K. O. Adebowale, *J. Hazard. Mater.*, **179**, 415 (2010).
45. P. Suksabye, P. Thiravetyan and W. Nakbanpote, *J. Hazard. Mater.*, **160**, 56 (2008).
46. Z. Aksu and F. Gonen, *Process. Biochem.*, **39**, 599 (2004).
47. Y. Fu and T. Viraraghavan, *Water SA*, **29**, 465 (2003).
48. E. Malkoc, Y. Nuhoglu and Y. Abali, *Chem. Eng. J.*, **119**, 61 (2006).
49. J. R. Rao and T. Viraraghavan, *Bioresour. Technol.*, **85**, 165 (2002).
50. A. D. Easton, L. S. Clesceri and A. E. Greenberg, *Standard methods for the examination of water and wastewater, Standard Methods*, (APHA, AWWA, WEF) 17th Ed. (1989).
51. M. C. Huang, C. H. Chou and H. Teng, *AIChE J.*, **48**, 1804 (2002).
52. Z. Aksu, S. S. Cagatay and F. Gonen, *J. Hazard. Mater.*, **143**, 362 (2007).
53. S. Singha, U. Sarkar, S. Mondal and S. Saha, *Desalination*, **297**, 48 (2012).
54. S. Saha, U. Sarkar and S. Mondal, *Desali. Water Treat.*, **37**, 277 (2012).